Oligodendroglial maldevelopment in the cerebellum after postnatal hyperoxia and its prevention by minocycline

Till Scheuer[1,2,*], **Vivien Brockmöller**[1,*], **Marissa Blanco Knowlton**[3], **Jörn-Hendrik Weitkamp**[3], **Torben Ruhwedel**[4], **Susanne Mueller**[5], **Stefanie Endesfelder**[1], **Christoph Bührer**[1], and **Thomas Schmitz**[1]

[1]Department for Neonatology, Technische Universität Berlin, 13353 Berlin, Germany

[2]Institute of Bioanalytics, Technische Universität Berlin, 13353 Berlin, Germany

[3]Vanderbilt University, Department of Pediatrics, Nashville, TN, USA

[4]Max-Planck-Institute of Experimental Medicine, Department of Neurogenetics, Göttingen, Germany

[5]Center for Stroke Research, Charité University Medical Center, Berlin, Germany

Abstract

According to recent research, brain injury after premature birth often includes impaired growth of the cerebellum. However, causes of cerebellar injury in this population are poorly understood. In this study, we analyzed whether postnatal hyperoxia perturbs white matter development of the cerebellum, and whether cerebellar glial damage can be prevented by minocycline.

We used a hyperoxia model in neonatal rats providing 24h exposure to 4-fold increased oxygen concentration (80% O_2) from P6 to P7, followed by recovery in room air until P9, P11, P15, P30. Injections with minocycline were performed at the beginning and 12h into hyperoxia exposure.

Hyperoxia induced oxidative stress in the cerebellum at P7 as evidenced by increased nitrotyrosine concentrations. Numbers of proliferating, NG2+Ki67+ oligodendroglial precursor cells were decreased at P7 after hyperoxia and at P11 following recovery in room air. Numbers of mature, CC1+ oligodendrocytes were diminished in recovering hyperoxia rats, and MBP expression was still decreased at P30. Electron microscopy analysis of myelinated fibers at P30 revealed thinner myelin sheath after hyperoxia. Long-term injury of the cerebellum by neonatal hyperoxia was confirmed by reduced volumes in MRI measurements at P30. In response to 80% O_2, expression of PDGF-A was largely reduced in cerebellar tissue and also in cultured cerebellar astrocytes. Treatment with minocycline during hyperoxia prevented oxidative stress, attenuated oligodendroglial injury, and improved astroglial PDGF-A levels.

In conclusion, early hyperoxia causes white matter damage in the cerebellum with astroglial dysfunction being involved, and both can be prevented by treatment with minocycline.

Corresponding author: Dr. Thomas Schmitz, Klinik für Neonatologie, Charité Universitätsmedizin Berlin, Augustenburger Platz 1, Mittelallee 9, 13353 Berlin, Germany, Phone: +49 30 450 559548, FAX: +49 30 450 559979, thomas.schmitz@charite.de.
*Equal contribution of these authors.

Author Manuscript

Author Manuscript

Author Manuscript

Author Manuscript

INTRODUCTION

Preterm infants often suffer from impaired postnatal brain development leading to neurological deficits. Symptoms include poor memory and cognition, but also impaired motor coordination and balance (Riva and Giorgi, 2000; Larroque et al., 2008; de Kieviet et al., 2009; Stoodley and Schmahmann, 2009). In general, diffuse white matter damage (WMD) in association with hypomyelination is recognized as a major underlying pathology (Kinney, 2005; Miller et al., 2005; Folkerth, 2006; Constable et al., 2008; Back and Miller, 2014). While cystic lesions of the white matter predominantly result from ischemia (Back and Miller, 2014) diffuse WMD and hypomyelination in preterm infants have been associated with perinatal infection / inflammation (Dammann and Leviton, 2004; Kinney, 2005), hypocapnia (Leviton et al., 2010), and hyperoxia (Deulofeut et al., 2007; Gerstner et al., 2007). In addition, pathologies of the cerebellum have been recognized more recently in preterm infants, although causes are unclear (Volpe, 2009). A reduction of the cerebellar volume is frequently found in preterm infants (Limperopoulos et al., 2005) and may correlate with impaired neurological development at term gestation (Spittle et al., 2010), lower IQ scores at school age (Northam et al., 2011) and behavioral concerns at adolescence (Parker et al., 2008). Notably, WMD in the cerebellum may also impair cerebral development (Limperopoulos et al., 2010). While arterial oxygen tension *in utero* is maintained at low levels between 24–28 mmHg, premature birth into room air causes a several-fold increase in arterial oxygen tension in preterm infants to 65 mmHg and higher, even without supplemental oxygen (Castillo et al., 2008). The exposure to this hyperoxic *ex utero* environment affects the cerebellum during a phase of very dynamic growth and cellular development (Volpe, 2009). Immature oligodendroglial lineage cells in particular show a high vulnerability to oxidative stress (Back et al., 1998; Baud et al., 2004; Schmitz et al., 2011), leading to increased apoptotic cell death (Gerstner et al., 2006), decreased proliferation (Schmitz et al., 2011), and perturbed maturation of oligodendroglial precursor cells (OPCs) (Ritter et al., 2013).

Oligodendroglia cell development is regulated by complex glia-glia interactions. Microglia and astrocytes express supporting factors that are essential for the survival, proliferation and maturation of OPCs (Wilson et al., 2003; Clemente et al., 2013; Hill et al., 2013). The expression of cytokines by microglia also influences oligodendroglial development (Benn et al., 2001; Pang et al., 2005; di Penta et al., 2013), and imbalance caused by microglial activation may be detrimental for myelination and white matter integrity.

In this study, we aimed to investigate how postnatal exposure to high oxygen levels affects oligodendroglial development of the cerebellum and if pathologies in microglia and astroglia are involved. Moreover, we tested whether treatment with the pleiotropic drug minocycline exerts benefits on the immature cerebellar white matter. The results deliver new insights into cellular mechanisms that are critical for injury or protection of the immature cerebellum.

MATERIALS AND METHODS

Animals and hyperoxia exposure

All animal experiments were performed in accordance with international guidelines for good laboratory practice and were approved by the animal welfare committees of Berlin, Germany. Six days old (P6) Wistar rats were subjected to 24h hyperoxia (80% O_2) until P7. Litters were divided into the three experimental groups of hyperoxia, hyperoxia with minocycline administration, and control pups. Newborn rats exposed to hyperoxia were placed along with their mothers, in a chamber containing 80% O_2 (OxyCycler, BioSpherix, Lacona, NY, USA). It has previously been reported in this rodent model, exposure to 80% oxygen causes a three- to fourfold increase of oxygen tension to values of 155 to 182 mmHg (Felderhoff-Mueser et al., 2004; Schmitz et al., 2011). Body weight of P7 pups was similar in both groups, health state and breeding behavior of mothers was not affected by hyperoxia. Minocycline was injected intra-peritoneally (i.p.) at the beginning and 12h into exposure to hyperoxia. The control pups of each litter were kept in room-air with a second lactating mother. During recovery in room air, all pups exposed to hyperoxia were reunited with their biological mother until further testing. The pups exposed to hyperoxia appeared normal and did not suffer weight loss or other morbidities, irrespective of minocycline treatment.

MRI volume measurement

For determination of cerebellar volumes by T2w MRI we used a 7 Tesla rodent scanner (Pharmascan 70/16, Bruker BioSpin, Ettlingen, Germany) with a 16 cm horizontal bore magnet and a 9 cm (inner diameter) shielded gradient. Imaging was performed with a 72-mm-volume resonator for transmission and a ^{1}H-Phased-Array mouse head surface coil (both Rapid Biomed, Rimpar, Germany) for reception. During the examinations, rats were placed on a heated circulating water blanket to ensure constant body temperature of 37 °C. Anaesthesia was induced with 3% and maintained with 1.5–2.0% isoflurane (Forene, Abbot, Wiesbaden, Germany) delivered in 0.5 L / min of 100% O2 via a facemask under constant ventilation monitoring (Small Animal Monitoring & Gating System, SA Instruments, Stony Brook, New York, USA). T2-weighted imaging was acquired with a 2D turbo spin-echo sequence with fat suppression (imaging parameter: TR / TE = 4200 / 36 ms, RARE factor 8, 4 averages, scan time 6min 43s). 25 sagittal slices with a slice thickness of 0.5 mm, a field of view of 2.85×2.85 cm and a matrix size of 256×256 were positioned over the whole brain. Calculation of each cerebellum volume was carried out with the program Analyze 5.0 (AnalyzeDirect, Inc.; Lenexa USA). The corresponding structures in T2-weighted images were assigned with a region of interest tool. This results in a 3D object map of the whole cerebellum which was automatically calculated.

Immunofluorescence

Rats at P7, P9, P11, P15 and P30 were anesthetized following animal welfare committee guidelines, transcardially perfused with PBS followed by 4% paraformaldehyde (PFA). Cerebellums were dissected, fixed with 4% PFA overnight at 4°C, paraffin embedded and processed for histological staining. Sections were cut at 5–10 μm and stored at room temperature. For immunohistochemistry, sections were proceeded as previously described (Endesfelder et al., 2013). Polyclonal mouse antibody to NG2 chondroitin sulfate

proteoglycan (Chemicon, Temecula CA) was diluted 1:500. Monoclonal mouse antibody to myelin basic protein (MBP) (Covance, VA) was diluted 1:500. The monoclonal rabbit Ki67 antibody (Leica Biosystems, Newcastle, UK) was diluted 1:200. Monoclonal mouse CC1 antibody was diluted 1:500 (Abcam, Cambridge MA; Calbiochem, Darmstadt, Germany). Rabbit Iba1 antibody (Wako Chemicals, Richmond VA) was diluted 1:750. All secondary antibodies used were from Jackson Immunoresearch Laboratories, West Grove PA, in carrier solution: FITC-conjugated goat anti-mouse IgG (1:200), FITC-conjugated goat anti-rabbit IgG (1:200), CY3/Rhodamine conjugated goat anti-mouse IgG (1:200) and CY3/Rhodamine conjugated goat anti-rabbit IgG (1:200). Stained sections were mounted in Vectashield mounting medium containing DAPI.

Cell cultures

Primary mixed glial cultures were prepared from E19 pregnant Sprague-Dawley rats by mechanical dissociation according to the method of McCarthy and de Vellis (McCarthy and de Vellis, 1980) as previously described (Gallo and Armstrong, 1995; Schmitz et al., 2011). To obtain microglia cell suspensions, mixed cultures (10–12 days old) were shaken for 2 h, and supernatants with detached microglia were used for microglia culture experiments. To obtain oligodendrocyte progenitor cells (OPC) suspensions, media of the mixed cultures was replaced before overnight shaking of the flasks. To minimize contamination by microglial cells, the detached cell suspension was incubated in succession for 45 min. each in 60 mm dishes. OPCs enriched by this method contained > 95% GD31 cells labeled by the LB1 monoclonal antibody (Curtis et al., 1988) with < 0.5% glial fibrillary acid protein (GFAP)+ astrocytes and < 0.5% Ox42$^+$ microglia. Attached astrocytes were passaged after overnight shaking and transferred into T75 culture flasks (BDFalcon, San José CA) at a density of 2×10^6 cells per flask with 10 ml DMEM media (Gibco Invitrogen, Carlsbad CA) containing 10% FCS which was changed after overnight incubation in order to remove non-attached OPCs. Once cells became confluent, flasks were shaken overnight and media containing non-attached OPCs and microglia was removed.

For quantitative real-time PCR analysis, astrocytes were plated after trypsinization on poly-lysine-coated 12 well plates in a density of 1.8×10^5 cells per well in 1 ml DMEM with 10% FCS. After 24h the medium was changed to DMEM containing 1% FCS. The 12 well plates were then used for experiments at 80 % and at 21 % oxygen. Cells for minocycline experiments were pre-incubated with 10μM minocycline for 1h. After 24h incubation cells were lysed for RNA isolation.

TUNEL Assays

Rhodamine-dUTP TUNEL assays were performed according to the manufacturer's directions (In Situ Cell Death detection kit, Rhodamine, Roche Applied Science, Indianapolis IN). TUNEL immunostaining was performed on tissue dissected following hyperoxia (with and without minocycline treatment) or from animals kept in room air (control). Tissue was then processed for NG2 immunolabeling as previously described (Schmitz et al., 2014) above (Immunofluorescence). Sections were then permeabilized using 0.2% Triton X-100 in 1xPBS for 1 hour, rinsed with 1xPBS and incubated with TUNEL

solution for 1 hour at 37°C. After 3 washes in 1xPBS, tissue was mounted with Vectashield containing DAPI.

Western blotting

Micro-dissected tissue of one hemisphere of the cerebellum was homogenized in 4°C RIPA buffer solution for protein extraction. Aliquots were then assayed for protein concentration using the Pierce BCA kit (Pierce, Rockford IL). Total proteins were equally loaded (10–40 μg per lane) on 4–20% mini precast Tris-glycine gels. The gels were transferred onto PVDF membranes at 4°C overnight and blocked in 3% BSA in TBST. Primary antibodies were diluted 1:500 to 1:2,000 in 3% BSA/TBST. Horseradish peroxidase (HRP)-conjugated secondary antibodies (anti-rabbit and anti-mouse, BD Biosciences Pharmingen, San Diego CA) were diluted 1:2,000 in 3% BSA/TBST. Chemiluminescent detection was performed using ECL Plus (Amersham) or Supersignal West Pico (Pierce) kits according to manufacturers' directions. The antibodies used were monoclonal mouse anti MBP 1:1000 (Covance VA), monoclonal mouse anti β-Actin 1:1250 (Millipore/Chemicon, Temecula CA), polyclonal rabbit anti Nitrotyrosine 1:1000 (Millipore/Upstate, Temecula CA).

RNA extraction and quantitative real-time PCR (qPCR)

Total RNA was isolated by acidic phenol/chloroform extraction (peqGOLDRNApure, PEQLAB Biotechnologie, Erlangen, Germany), and 2 μg of RNA were reverse transcribed. The cDNA was analyzed with primers for *Olig2, CNP, IGF1, PDGF-A, GFAP, TNF-α, IL-18,* and *HPRT* by qPCR, using dye-labeled fluorogenic reporter oligonucleotide probes with sequences as listed in Table 1. PCR and detection were performed in triplicate and repeated two times for each sample in 11 μl reaction mix containing 5 μl of 2x KAPA PROBE FAST qPCR Mastermix (PEQLAB Biotechnologie), 2.5 μl of 1.25 μM oligonucleotide primermix, 0.5 μl (0.5 μM) of probe (BioTeZ, Berlin, Germany) and 23 to 230 ng of cDNA template. *HPRT* was used as an internal reference. The expressions of target genes were analyzed with the StepOnePlus™ qPCR System (Applied Biosystems, Life Technologies, Carlsbad, CA) according to the 2^{-} CT method (Livak and Schmittgen, 2001).

Microscopy measurements

Zeiss LSM 510—A Zeiss LSM 510 confocal laser scanning microscopic (CLSM) system was used for the analysis of fluorescence following immunohistochemical staining in rats. Optical sections were acquired with field depth of 10 μm, using a 20× objective and the LSM 510 software. Three different laser lines were used to image localization of FITC (488 nm excitation; 522/35 emission filter), CY3 (560 nm excitation; 605/32 emission filter), and DAPI (400 nm excitation). Data acquisition and processing were controlled by LSM software. Analysis of immunofluorescence was performed on confocal *z*-stacks. Cells were counted in 225 X 225 X 10 μm (20X – *X, Y, Z* planes) images for cells/volume quantifications. An average of 3 images was taken from 3 different areas (from proximal to distal in one lobule) for 2–3 sections of each animal analyzed. Confocal Assistant 4.02 and Image J (National Institutes of Health, Bethesda, MD, USA) software were used to merge images for analysis. Merged images were processed in Photoshop CSM with minimal

manipulation of contrast. Cells were counted in a blinded fashion and double or triple labeled by analyzing the merged image for each confocal *z*-stack and identifying positive immunofluorescence for each individual channel. For morphometric analysis, confocal z-stacks were converted into 2-dimensional images using maximum intensity projection algorithm, and after segmentation according to fluorescence intensity, cell areas and perimeters were measured with Image J software.

Leica DM 2000—Immunohistochemical stained cerebellar sections for MBP, CC1 and GFAP were analyzed using a Leica DM 2000 microscope with a 10× and 20× Objective, and the Leica Application Suite-LAS software (Leica Microsystems, Wetzlar, Germany). We analyzed the pixel intensity of 3 pictures of each animal using ImageJ (National Institutes of Health, Bethesda, MD, USA).

Electron microscopy—Rats were anesthesized and received transcardial perfusion with a 0.1 M phosphate buffer saline followed by fixative containing 4 % formaldehyde, 2.5 % glutaraldehydeand 0.5% NaCl in phosphate buffer pH 7.4 according to Karlsson and Schultz (Karlsson and Schultz, 1965). To reduce myelin damage, each perfusion was done with an automated perfusion pump with a constant flow of 5 ml/h. Brains were then kept in the fixation buffer for 48 hours in a refrigerator at $4 - 8$ °C. Sagittal 200 μm vibratome sections of the cerebellum were postfixed with 2 % OsO_4 in 0.1 M phosphate buffer pH 7.3 and embedded in EPON after dehydration with ethanol and propylenoxide (Möbius et al., 2010). These were used to first collect thin sections of 0.5 μm and in a second step cut ultra-thin slices of 50 nm which were placed on grids and stained with uranyl acetate and lead citrate. The grids were then imaged using a transmission ZEISS electron microscope ("Leo 906", Jena, Germany). Randomly selected axons (80 – 100 per section of the cerebellum) were counted and classified. For one animal, 500 to 600 cerebellar axons were measured, with axons of < 0.2 μm excluded from the analysis. Parameters for analysis included whole fiber diameter (axon with myelin), inner axonal diameter, myelin sheath thickness, and G ratio as a result of inner axon diameter over outer diameter.

Statistics

Results are in general expressed as mean $+/-$ SEM, only for MRI median and quartiles are presented. For statistical analysis a one-way analysis of variance (ANOVA) was performed overall, followed by post-hoc t-test for paired groups. All graphics and statistical analyses were performed using the Graph Pad Prism 5.0 software.

RESULTS

Postnatal hyperoxia diminishes cerebellar growth until young adult ages

Since preterm infants show impaired development of the cerebellum with reduced volumes during later childhood (Limperopoulos et al., 2005), we measured cerebellar volumes by MRI in rats at ages P30 and P60 after postnatal exposure to hyperoxia (24 h from P6 to P7) in comparison to control litters always kept in room air (Fig. 1A,B) (n=6 each group). In control rats, cerebellar median volume was 230.3 mm³ (range: 216.1 – 235.1 mm³) at age P30, which increased to 297.2 mm³ (range: 266.5 – 327.4 mm³) at age P60, reflecting the

dynamic increase of cerebellar size during physiological postnatal development (Fig. 1C). The results for cerebellar volumes obtained in our P30 control rats were similar to those data reported by Sawada in 4 week old healthy rats (Sawada et al., 2013). In rats previously exposed to hyperoxia, cerebellar volume was significantly reduced to 208.4 mm^3 (range 201.7 to 220.2 mm^3) at age P30 (P<0.01) (Fig. 1C). Although hyperoxia-experienced rats showed cerebellar growth at P60 with a median volume of 262.3 mm^3 (range 228.8 – 275.9 mm^3), a significant volume reduction remained in comparison to age-matched controls (P<0.05) (Fig. 1C). Altogether, hyperoxia in newborn rats induced a cerebellar volume deficit that mimics findings in preterm infants (Limperopoulos et al., 2005).

To analyze protection against hyperoxia-induced cerebellar injury, we administered minocycline to P6 rat pups at the beginning and 12 h into hyperoxia exposure. As a result, hyperoxic rats treated with minocycline had significant improvement of cerebellar volume in comparison to hyperoxia litters, both at P30 (median 220.4, range 206.0 mm^3 – 231.2 mm^3) (P<0.05) and at P60 (median 287.4, range 266.8 mm^3 – 308.8 mm^3) (P<0.01) (Fig. 1C). In fact, cerebellar volumes in minocycline treated rats with hyperoxia exposure were not different to normal controls (Fig 1C). These results indicate that minocycline can protect the immature cerebellum against maldevelopment caused by hyperoxia.

Hyperoxia causes oxidative stress in cerebellar tissue and induces apoptosis in oligodendroglia precursor cells (OPCs), which can be attenuated by minocycline

Damage of the immature white matter often implies diminished survival of oligodendroglial lineage cells as has been demonstrated in injury models of hypoxia–ischemia and hypoglycemia in newborn rats (Back et al., 1998; Yan and Rivkees, 2006). High oxygen levels, in particular, can result in apoptotic cell death of neural cells and OPCs in the cerebrum of newborn rats and mice (Felderhoff-Mueser et al., 2004; Schmitz et al., 2011; Vottier et al., 2011). Whether and to which extent it may also cause oligodendroglial injury and WMD in the cerebellum has not been shown yet.

To investigate whether hyperoxia causes oxidative stress in the postnatal cerebellum, we used cerebellar hemisphere protein lysates for Western blot analysis with antibodies against nitrotyrosine. As a result, levels of nitrotyrosine were increased 2.6-fold in cerebellar lysates of rats exposed to 24 h hyperoxia from P6 to P7 (Fig. 2C,D). In contrast, minocycline blocked the increase of nitrotyrosine under hyperoxic conditions.

For analysis of apoptosis in OPCs, we performed immunohistochemistry with TUNEL and NG2 immunostaining in cells located in white matter tracts of the cerebellar lobules. An increased number of apoptotic, NG2+TUNEL+ OPCs were found in P7 rats after 24 h of hyperoxia, and also after two days and four days recovery in room air at P9 and at P11 (Fig. 2A,B). Treatment of rats with minocycline prevented hyperoxia-induced apoptosis in OPCs at P7 and at P9. Later at P11, however, no significant protection against apoptosis was found in hyperoxia rats (Fig. 2A,B).

Minocycline improves proliferation and maturation of OPCs in the cerebellum of hyperoxic rats

OPCs and immature oligodendroglia undergo an intensive period of proliferation until they become mature oligodendrocytes (Reynolds and Wilkin, 1988; Gallo et al., 1996; Emery, 2010). To investigate the effects of hyperoxia on OPC proliferation and to test for benefits of minocycline treatment, we labeled OPCs with NG2 and Ki67 by immunohistochemistry. At P7 after 24 h of hyperoxia, numbers of proliferating (i.e., NG2+Ki67+) OPCs in the cerebellar white matter were significantly diminished in comparison to control rats (Fig. 3A). Notably, this deficit in proliferating OPCs persisted after withdrawal of hyperoxia at ages P9 and P11 (Fig. 3B). Hyperoxic rats with minocycline did not show decreased proliferation of OPCs (Fig. 3A,B). In accordance with these findings, the total numbers of NG2+ OPCs were significantly diminished at ages P9 and P11 hyperoxia-experienced rats (Fig. 3C).

To assess maturation of oligodendroglial lineage cells, we determined the numbers of mature, CC1 expressing oligodendrocytes by immunohistochemistry at ages P7, P9 and P11. As a result, the numbers of CC1+ mature oligodendrocytes were similar in all three experimental groups at age P7. During further development, an expansion of the mature oligodendrocyte population was obvious in control rats at P9 and at P11. However, rats exposed to hyperoxia followed by recovery in room air until P9 and until P11 were lacking this maturational progress and showed a significant reduction of CC1+ cells compared to control rats (Fig. 4A,B). In contrast, reduction of mature oligodendrocytes after hyperoxia was not found in rats treated with minocycline (Fig. 4A,B).

We also analyzed gene expression of the oligodendroglial transcription factor Olig2 and of the maturational marker 2′,3′-cyclic-nucleotide 3′-phosphodiesterase (CNP) by qPCR. Both Olig2 expression and CNP expression were lower in P7 rats exposed to hyperoxia (Fig. 4C,D). At P11, expression levels of Olig2 and CNP in hyperoxia experienced rats returned to control levels (Fig. 4C,D), although this normalization was apparently not sufficient to compensate the previous deficits as indicated by the aforementioned persistence of CC1+ reduction. P7 rats treated with minocycline during hyperoxia had significant higher gene expression levels of Olig2 and CNP compared to hyperoxic rat pups without treatment.

Minocycline improves myelination of the cerebellum after hyperoxia

A major function of mature oligodendrocytes is the myelination of axons by formation of myelin sheaths in order to increase conduction of nerve impulses (Baumann and Pham-Dinh, 2001). To investigate the impact of hyperoxia and minocycline on myelination in the cerebellum, we quantified the expression of MBP and analyzed the ultrastructure of myelinated fibers.

MBP expression was measured by Western blot after exposure to hyperoxia, at ages P9, P11, P15, and P30 (Fig. 5A,B). At P7, the amount of MBP was too low even in control animals to be quantified reliably, but starting from P9, there was a significant hyperoxia-induced deficiency of MBP at all ages until at least P30 (Fig. 5A,B). During recovery, there was a clear raise of MBP formation even in hyperoxia rats, but never reaching control levels.

Based on these data, intermittent hyperoxia at neonatal ages caused a maturational delay of oligodendroglial cells that persists until young adult age and causes long-term myelin deficit. Notably, rats treated with minocycline during exposure to hyperoxia showed improved myelin synthesis at all ages investigated, even though MBP levels still tended to be lower than in controls at some of the time points (Fig. 5B).

In juvenile rats at P30, we also analyzed MBP formation in the cerebellum with immunohistochemistry. At the distal part of cerebellar lobules, fluorescence intensity was lower in hyperoxic rats compared to controls, confirming hyperoxia-induced MPB deficiency at this age. The protective effect of minocycline administration was supported by this analysis (Fig. 5C,D).

For ultrastructure analysis of myelinated axons in the cerebellum, we performed electron microscopy in rats at age P30. Images were taken from sagittal section of central white matter areas of the cerebellum to obtain radial presentation of the fibers and measure diameters of inner axons and of myelin sheaths (Fig. 6A). As a result, the mean fiber size was significantly reduced in P30 rats following postnatal hyperoxia (Fig. 6B). Minocycline treatment during exposure to hyperoxia improved the mean fiber size compared to the hyperoxia group (Fig. 6B). There was a trend for reduction in mean axon size measured as inner fiber diameter without the myelin sheath (p=0.06) (Fig. 6C). This trend did not exist in rats treated with minocycline (Fig. 6C). More clearly, a pronounced thinning of the myelin sheath was obtained in rats after hyperoxia, which was also expressed by increased G ratios in these animals (Fig. 6D,E). Minocycline blocked the changes found in the myelin sheath and in the G ratio (Fig. 6D,E).

Changes in cerebellar glia-glia interactions after hyperoxia

The synthesis of growth factors and cytokines by microglia and astroglia has strong influences on the development of oligodendroglia and on myelination (Benn et al., 2001; Wilson et al., 2003; Back and Rosenberg, 2014). Insulin-like growth factor-1 (IGF1) secreted by microglia is important for proliferation and maturation of OPCs (Wilson et al., 2003; Clemente et al., 2013). Moreover, IGF1 has been shown to be protective in oligodendroglia exposed to inflammatory stimuli (Pang et al., 2007). Increased release of pro-inflammatory cytokines, such as TNFα, by activated microglia leads to oligodendroglial maldevelopment (Benn et al., 2001; Pang et al., 2005; di Penta et al., 2013), and microglial inhibition by minocycline seems to be beneficial (Fan et al., 2005; Defaux et al., 2011). Injections of IL-1β in newborn rats caused severe and persistent hypomyelination until adulthood (Favrais et al., 2011).

To test for activation and morphological changes of microglia in our experiments, we performed immunohistochemistry for Iba1 in the cerebellum at P7 and P11. As a result, hyperoxia had no detectable effect on the shape of Iba1+ microglia, and Iba1+ staining intensity was similar in hyperoxic rats and in controls at both ages (suppl. Fig. A). In all three experimental groups at P7, Iba1+ microglia show similar ameboid shape and an intermediate to ramified configuration at P11 (suppl. Fig. A,B). Moreover, gene expression analysis of the cytokines TNF-α and IL-1β showed similar levels in the rat cerebellums in all experimental groups at P7 (suppl. Fig. D,E). At P11, an increase of TNF-α was found in the

cerebellum of rats following hyperoxia, which was abolished by minocycline (suppl. Fig. E). IL-1β gene expression was not altered at P11 (suppl. Fig. D). Expression levels of IL-18 and of MHC-II did not change after hyperoxia (data not shown). Levels of IGF1 gene expression were similar in hyperoxia rats and in controls at P7 and at P11 (suppl. Fig. C). In minocycline-treated rats there was a decrease of IGF1 expression at P11. Altogether, we did not find signs of broad microglial activation immediately after exposure to hyperoxia at P7 and only partial changes after recovery at P11, hence contrasting results previously obtained in the corpus callosum which indicated acute microglial activation caused by hyperoxia (Schmitz 2014).

A lack of platelet-derived growth factor-A (PDGF-A) expression in knockout mice leads to severe oligodendroglial impairment and hypomyelination in the cerebellum (Fruttiger et al., 1999). PDGF-A directly regulates proliferation and survival of OPCs (Fruttiger et al., 1999; Clemente et al., 2013; Hill et al., 2013; Funa and Sasahara, 2014), and astrocytes have been shown to secret PDGF-A to stimulate OPC proliferation (Besnard et al., 1987; Raff et al., 1988; Richardson et al., 1988; Gard et al., 1995; Clemente et al., 2013). In order to investigate a role of altered growth factor expression for oligodendroglial injury caused by hyperoxia, we measured PDGF-A gene expression levels in cerebellum samples at P7 and P11. We found that expression of PDGF-A was markedly downregulated by hyperoxia to 66% of control levels at P7, and even more pronounced to 34% of control levels after four days of room air recovery at P11 (Fig. 7A). The reduction of astroglial PDGF-A was confirmed in culture experiments using primary cerebellar rat astroglia *in vitro* (Fig. 7B). In these cultures, 4-fold increase of oxygen by exposure to 80% O_2 for 24 h caused a decrease of PDGF-A expression to 56% as compared to that obtained under culture conditions with 21 % O_2. Minocycline improved PDGF-A expression in rats at P7 and at P11, and also in the cultured astroglia exposed to high oxygen *in vitro* (Fig. 7A,B). Since astroglial activation may imply changes in GFAP formation, we performed RNA expression analyses of cerebellar samples and GFAP immunostainings in the white matter of the cerebellum at P7 and at P11. However, there was no significant change of GFAP expression levels (Fig. 7C). Moreover, the morphology and the mean pixel intensity of GFAP+ astroglia in the white matter were not affected by hyperoxia (Fig. 7D,E).

These data in newborn rats indicate that high oxygen does not lead to a drastic astroglial activation or astrogliosis in the immature cerebellum but to a significant reduction of astroglial PDGF-A that may contribute to oligodendroglial maldevelopment.

DISCUSSION

In this study, we investigated the influence of postnatal hyperoxia on cerebellar white matter development. In addition to overall reduced cerebellar volumes at young adult ages, we found that OPCs underwent increased apoptosis, reduced proliferation, and maturational delay after hyperoxia. Moreover, astroglia had diminished production of PDGF-A indicating perturbed glia-glia interactions by hyperoxia. Altogether, the pathological features of the cerebellum obtained after neonatal hyperoxia seem to mimic important features of cerebellar WMD that have been described in former preterm infants (Limperopoulos et al., 2005, 2010).

From 24 weeks to 40 weeks of gestation, the cerebellum undergoes dramatic developmental changes and increases its volume 5-fold. In preterm infants, the cerebellum is exposed to various environmental stimuli at early stages of this vulnerable phase. In fact, preterm birth increases the risk for cerebellar maldevelopment, but the underlying mechanism is unclear (Limperopoulos et al., 2005, 2010; Volpe, 2009; Haldipur et al., 2011). In the past, the cerebellum was viewed as a processor that uses a variety of inputs to guide movements (Wang et al., 2014). In contrast, recent studies have indicated that the cerebellum is involved in a broad variety of complex processes, including cognition and learning behavior (Steinlin, 2008; Stoodley et al., 2012), and that it plays a role in psychiatric disorders such as attention-deficit/hyperactivity disorder (ADHD) and autism (Fatemi et al., 2009; Ivanov et al., 2014; Wang et al., 2014).

In our rat model, oligodendroglial injury induced by hyperoxia was characterized by reduced numbers of OPCs as a result of decreased proliferation and enhanced apoptosis that persisted after withdrawal of the hyperoxic stimulus. In previous studies in the rodent subcortical white matter, it had been shown that during recovery, a compensation of oligodendroglial proliferation occurs to levels even beyond those of controls (Schmitz et al., 2011, 2014). In rodent brain injury models using different postnatal stimuli, repair of the oligodendroglial population could be characterized as the result of local recovery in the white matter and of recruitment of OPCs from the subventricular zone (Fagel et al., 2006; Maki et al., 2013). Based on our data in this study, the capacity of spontaneous repair is less pronounced in the white matter of the cerebellum as compared to the cerebrum. In concordance with the results obtained in previous studies of the cerebrum (Gerstner et al., 2006; Schmitz et al., 2011), mature (CC1+) oligodendrocytes in the cerebellum were not degenerated during or immediately after the exposure to hyperoxia, but expansion of the mature CC1+ oligodendrocyte population during ongoing development was largely reduced.

The impairment of oligodendroglial development and maturation resulted in a long-term reduction of MBP expression. Ultrastructure analysis by electron microscopy indicated a decreased thickness of the myelin sheath wrapped around the axon. In contrast to ultrastructural changes found in the cerebral white matter in mice after hyperoxia (Ritter et al., 2013), axon diameters were not strongly affected in this study. Axonopathy has been reported in an inflammatory injury model applying injections of IL-1β over five days postnatally (Favrais et al., 2011), and the role of axonopathy in white matter injury of preterm infants has been discussed (Leviton et al., 2010). To our knowledge, axonal injury has not been reported in neonatal injury models of the cerebellum. Our data indicate that a short exposure to a rather mild stimulus as represented in our hyperoxia model may cause only minor axonopathy in the cerebellum.

Glial cell signaling is indispensable for proper oligodendroglial development (Clemente et al., 2013). Survival, proliferation and maturation of OPCs is influenced by a number of growth factors and cytokines (Benn et al., 2001; Wilson et al., 2003; Back and Rosenberg, 2014). Astrocytes express PDGF-A to promote OPC proliferation (Clemente et al., 2013; Hill et al., 2013; Funa and Sasahara, 2014). In our experiments, we found markedly reduced PDGF-A expression in the cerebellum after hyperoxia *in vivo*. The fact that the reduction of PDGF-A expression by high oxygen levels was confirmed in purified astrocyte cultures *in*

vitro points to a possible impairment of astroglia-oligodendroglia-crosstalk in cerebellar injury after hyperoxia. Notably, astroglial morphology and GFAP expression were not affected by hyperoxia. The protection of cerebellar white matter development by minocycline was associated with improved PDGF-A expression *in vivo* and in astrocyte cultures *in vitro*, underlining a role for astroglial PDGF-A both in injury and protection in the cerebellum.

Production of cytokines and growth factors by microglia are needed for healthy oligodendroglial development (Wilson et al., 2003; Pang et al., 2007; Clemente et al., 2013). In the human embryo, colonization of the forebrain with microglia occurs at around 5 gestational weeks, while in rats this event takes place at embryonic day 11 (Ashwell, 1991). Ramification as a process of microglial maturation occurs in the human mesencephalon between 11 and 22 gestational weeks, whereas in the cerebellum, the immature ameboid shape maintains to the predominant microglial phenotype much longer (Wierzba-Bobrowicz et al., 1998). In accordance with the physiologically delayed maturation of microglia in the cerebellum, most of the Iba1+ cells in the cerebellar white matter in postnatal rats aged P7 to P11 were of ameboid morphology in our study, both in room air control pups and in hyperoxia-experienced litters. Microglial activation with enhanced release of cytokines and inflammatory mediators is described to impair oligodendroglial survival and maturation in models of inflammatory neonatal brain injury and of multiple sclerosis (Bannerman et al., 2007; Pinato et al., 2013) Activation of microglia often involves changes of morphology from ramified to ameboid, increased expression of adhesion molecules and immunological receptors, activation of receptor pathways, release of inflammatory cytokines and of radicals (Kettenmann et al., 2011). In the immature brain, microglial activation and inflammation may cause acute white matter injury (Back and Rosenberg, 2014) and persistent hypomyelination (Favrais et al., 2011). In our studies, we did not detect overt signs of broad microglial activation as determined by morphology, by expression of cytokines IL-1β, IL-18, TNFα, and by expression of IGF1 and MHC-II. However, we cannot exclude that other compounds, i.e. peroxides and radicals, could be released by microglia that might contribute to oxidative stress and oligodendroglial maldevelopment after hyperoxia. Similarly, more subtle responses with immune receptor pathway activation or transmitter releases have not been examined in our study. However, based on our data, a pronounced pro-inflammatory activation of microglia seems unlikely to occur in hyperoxia-induced cerebellar white matter injury.

Besides its antibacterial activity, minocycline has been demonstrated to exert neuroprotective properties in various models of brain injury, including hypoxia–ischemia (Arvin et al., 2002; Cai et al., 2006; Tang et al., 2010), perinatal inflammation/infection (Fan et al., 2005; Cai et al., 2010) and hyperoxia (Schmitz et al., 2014). The mechanisms by which minocycline exerts its benefits have largely been ascribed to inhibition of microglia. In the immature brain, inhibition of microglia may in fact perturb neuronal development and survival (Ueno et al., 2013). Toxic effects have been reported to vary with species, i.e. in mice, minocycline enhances brain injury caused by hypoxia-ischemia (Tsuji et al., 2004) application of minocycline. A deleterious response to minocycline has also been described in mouse models of Parkinson's disease and Huntington's disease (Diguet et al., 2004).

Extensive safety analysis of minocycline administration in the immature brain should therefore be a primary subject of distinct translational studies. In our study, oxidative stress was associated with exposure to hyperoxia and with cerebellar injury. Moreover, protection by minocycline coincided with attenuation of oxidative stress and of apoptotic cell death, which is supporting previous results on anti-oxidant and anti-apoptotic effects of minocycline (Xue et al., 2010).

In summary, our study demonstrates that postnatal hyperoxia causes oligodendroglial injury and hypomyelination in the cerebellum similar to the sequelae observed after preterm birth. It is noteworthy that based on the parameters examined in our study, we did not detect overt microglial activation in the cerebellum, and there were no signs of spontaneous repair in the oligodendroglial population during recovery, both of which are in contrast to the results previously obtained for the cerebrum. Interestingly, beneficial effects of minocycline administration in the cerebellum include improvement of astroglial growth factor synthesis. In our view, it is important to further investigate the developing cerebellum to deepen the understanding of its distinct pathways of injury and specific ways of protection.

Supplementary Material

Refer to Web version on PubMed Central for supplementary material.

Acknowledgments

Abbreviations

CBL	cerebellum
IL	interleukin
MBP	myelin basic protein
MRI	magnet resonance imaging
NGS	normal goat serum
Olig2	Oligodendrocyte transcription factor 2
OPC	oligodendroglial precursor cell
PDGF	Platelet-derived growth factor
PFA	paraformaldehyde
ROI	region of interest
TNF	tumor necrosis factor

TUNEL	Terminal deoxynucleotidyl-transferased UTP nick end labeling
WM	white matter
WMD	white matter damage

References

Arvin KL, Han BH, Du Y, Lin S, Paul SM, Holtzman DM. Minocycline markedly protects the neonatal brain against hypoxic-ischemic injury. Ann Neurol. 2002; 52:54–61. [PubMed: 12112047]

Ashwell K. The distribution of microglia and cell death in the fetal rat forebrain. Brain Res Dev Brain Res. 1991; 58:1–12. [PubMed: 2015649]

Back SA, Gan X, Li Y, Rosenberg PA, Volpe JJ. Maturation-dependent vulnerability of oligodendrocytes to oxidative stress-induced death caused by glutathione depletion. J Neurosci. 1998; 18:6241–6253. [PubMed: 9698317]

Back SA, Miller SP. Brain injury in premature neonates: A primary cerebral dysmaturation disorder? Ann Neurol. 2014; 75:469–486. [PubMed: 24615937]

Back SA, Rosenberg PA. Pathophysiology of glia in perinatal white matter injury. Glia. 2014; 62:1790–1815. [PubMed: 24687630]

Bannerman P, Hahn A, Soulika A, Gallo V, Pleasure D. Astrogliosis in EAE spinal cord: derivation from radial glia, and relationships to oligodendroglia. Glia. 2007; 55:57–64. [PubMed: 17009237]

Baud O, Haynes RF, Wang H, Folkerth RD, Li J, Volpe JJ, Rosenberg PA. Developmental up-regulation of MnSOD in rat oligodendrocytes confers protection against oxidative injury. Eur J Neurosci. 2004; 20:29–40. [PubMed: 15245476]

Baumann N, Pham-Dinh D. Biology of oligodendrocyte and myelin in the mammalian central nervous system. Physiol Rev. 2001; 81:871–927. [PubMed: 11274346]

Benn T, Halfpenny C, Scolding N. Glial cells as targets for cytotoxic immune mediators. Glia. 2001; 36:200–211. [PubMed: 11596128]

Besnard F, Perraud F, Sensenbrenner M, Labourdette G. Platelet-derived growth factor is a mitogen for glial but not for neuronal rat brain cells in vitro. Neurosci Lett. 1987; 73:287–292. [PubMed: 3561869]

Cai Z, Lin S, Fan L-W, Pang Y, Rhodes PG. Minocycline alleviates hypoxic-ischemic injury to developing oligodendrocytes in the neonatal rat brain. Neuroscience. 2006; 137:425–435. [PubMed: 16289838]

Cai Z-Y, Yan Y, Chen R. Minocycline reduces astrocytic reactivation and neuroinflammation in the hippocampus of a vascular cognitive impairment rat model. Neurosci Bull. 2010; 26:28–36. [PubMed: 20101270]

Castillo A, Sola A, Baquero H, Neira F, Alvis R, Deulofeut R, Critz A. Pulse oxygen saturation levels and arterial oxygen tension values in newborns receiving oxygen therapy in the neonatal intensive care unit: is 85% to 93% an acceptable range? Pediatrics. 2008; 121:882–889. [PubMed: 18450890]

Clemente D, Ortega MC, Melero-Jerez C, de Castro F. The effect of glia-glia interactions on oligodendrocyte precursor cell biology during development and in demyelinating diseases. Front Cell Neurosci. 2013; 7:268. [PubMed: 24391545]

Constable RT, Ment LR, Vohr BR, Kesler SR, Fulbright RK, Lacadie C, Delancy S, Katz KH, Schneider KC, Schafer RJ, Makuch RW, Reiss AR. Prematurely born children demonstrate white matter microstructural differences at 12 years of age, relative to term control subjects: an investigation of group and gender effects. Pediatrics. 2008; 121:306–316. [PubMed: 18245422]

Curtis R, Cohen J, Fok-Seang J, Hanley MR, Gregson NA, Reynolds R, Wilkin GP. Development of macroglial cells in rat cerebellum. I. Use of antibodies to follow early in vivo development and migration of oligodendrocytes. J Neurocytol. 1988; 17:43–54. [PubMed: 3047324]

Dammann O, Leviton A. Inflammatory brain damage in preterm newborns–dry numbers, wet lab, and causal inferences. Early Hum Dev. 2004; 79:1–15. [PubMed: 15282118]

Defaux A, Zurich M-G, Honegger P, Monnet-Tschudi F. Minocycline promotes remyelination in aggregating rat brain cell cultures after interferon-γ plus lipopolysaccharide-induced demyelination. Neuroscience. 2011; 187:84–92. [PubMed: 21549181]

Deulofeut R, Dudell G, Sola A. Treatment-by-gender effect when aiming to avoid hyperoxia in preterm infants in the NICU. Acta Paediatr. 2007; 96:990–994. [PubMed: 17577339]

Diguet E, Fernagut P-O, Wei X, Du Y, Rouland R, Gross C, Bezard E, Tison F. Deleterious effects of minocycline in animal models of Parkinson's disease and Huntington's disease. Eur J Neurosci. 2004; 19:3266–3276. [PubMed: 15217383]

Emery B. Regulation of oligodendrocyte differentiation and myelination. Science. 2010; 330:779–782. [PubMed: 21051629]

Endesfelder S, Zaak I, Weichelt U, Bührer C, Schmitz T. Caffeine protects neuronal cells against injury caused by hyperoxia in the immature brain. Free Radic Biol Med. 2013; 67C:221–234. [PubMed: 24129198]

Fagel DM, Ganat Y, Silbereis J, Ebbitt T, Stewart W, Zhang H, Ment LR, Vaccarino FM. Cortical neurogenesis enhanced by chronic perinatal hypoxia. Exp Neurol. 2006; 199:77–91. [PubMed: 15916762]

Fan L-W, Pang Y, Lin S, Tien L-T, Ma T, Rhodes PG, Cai Z. Minocycline reduces lipopolysaccharide-induced neurological dysfunction and brain injury in the neonatal rat. J Neurosci Res. 2005; 82:71–82. [PubMed: 16118791]

Fatemi SH, Folsom TD, Reutiman TJ, Thuras PD. Expression of GABA(B) receptors is altered in brains of subjects with autism. Cerebellum. 2009; 8:64–69. [PubMed: 19002745]

Favrais G, van de Looij Y, Fleiss B, Ramanantsoa N, Bonnin P, Stoltenburg-Didinger G, Lacaud A, Saliba E, Dammann O, Gallego J, Sizonenko S, Hagberg H, Lelièvre V, Gressens P. Systemic inflammation disrupts the developmental program of white matter. Ann Neurol. 2011; 70:550–565. [PubMed: 21796662]

Felderhoff-Mueser U, Bittigau P, Sifringer M, Jarosz B, Korobowicz E, Mahler L, Piening T, Moysich A, Grune T, Thor F, Heumann R, Bührer C, Ikonomidou C. Oxygen causes cell death in the developing brain. Neurobiol Dis. 2004; 17:273–282. [PubMed: 15474364]

Folkerth RD. Periventricular leukomalacia: overview and recent findings. Pediatr Dev Pathol. 2006; 9:3–13. [PubMed: 16808630]

Fruttiger M, Karlsson L, Hall AC, Abramsson A, Calver AR, Boström H, Willetts K, Bertold CH, Heath JK, Betsholtz C, Richardson WD. Defective oligodendrocyte development and severe hypomyelination in PDGF-A knockout mice. Development. 1999; 126:457–467. [PubMed: 9876175]

Funa K, Sasahara M. The roles of PDGF in development and during neurogenesis in the normal and diseased nervous system. J Neuroimmune Pharmacol. 2014; 9:168–181. [PubMed: 23771592]

Gallo V, Armstrong RC. Developmental and growth factor-induced regulation of nestin in oligodendrocyte lineage cells. J Neurosci. 1995; 15:394–406. [PubMed: 7823144]

Gallo V, Zhou JM, McBain CJ, Wright P, Knutson PL, Armstrong RC. Oligodendrocyte progenitor cell proliferation and lineage progression are regulated by glutamate receptor-mediated K+ channel block. J Neurosci. 1996; 16:2659–2670. [PubMed: 8786442]

Gard AL, Burrell MR, Pfeiffer SE, Rudge JS, Williams WC. Astroglial control of oligodendrocyte survival mediated by PDGF and leukemia inhibitory factor-like protein. Development. 1995; 121:2187–2197. [PubMed: 7635062]

Gerstner B, Bührer C, Rheinländer C, Polley O, Schüller A, Berns M, Obladen M, Felderhoff-Mueser U. Maturation-dependent oligodendrocyte apoptosis caused by hyperoxia. J Neurosci Res. 2006; 84:306–315. [PubMed: 16673399]

Gerstner B, Sifringer M, Dzietko M, Schüller A, Lee J, Simons S, Obladen M, Volpe JJ, Rosenberg PA, Felderhoff-Mueser U. Estradiol attenuates hyperoxia-induced cell death in the developing white matter. Ann Neurol. 2007; 61:562–573. [PubMed: 17427919]

Haldipur P, Bharti U, Alberti C, Sarkar C, Gulati G, Iyengar S, Gressens P, Mani S. Preterm delivery disrupts the developmental program of the cerebellum. PLoS ONE. 2011; 6:e23449. [PubMed: 21858122]

Hill RA, Patel KD, Medved J, Reiss AM, Nishiyama A. NG2 cells in white matter but not gray matter proliferate in response to PDGF. J Neurosci. 2013; 33:14558–14566. [PubMed: 24005306]

Ivanov I, Murrough JW, Bansal R, Hao X, Peterson BS. Cerebellar morphology and the effects of stimulant medications in youths with attention deficit-hyperactivity disorder. Neuropsychopharmacology. 2014; 39:718–726. [PubMed: 24077064]

Karlsson U, Schultz RL. FIXATION OF THE CENTRAL NERVOUS SYSTEM FROM ELECTRON MICROSCOPY BY ALDEHYDE PERFUSION. I. PRESERVATION WITH ALDEHYDE PERFUSATES VERSUS DIRECT PERFUSION WITH OSMIUM TETROXIDE WITH SPECIAL REFERENCE TO MEMBRANES AND THE EXTRACELLULAR SPACE. J Ultrastruct Res. 1965; 12:160–186. [PubMed: 14289426]

Kettenmann H, Hanisch U-K, Noda M, Verkhratsky A. Physiology of microglia. Physiol Rev. 2011; 91:461–553. [PubMed: 21527731]

De Kieviet JF, Piek JP, Aarnoudse-Moens CS, Oosterlaan J. Motor development in very preterm and very low-birth-weight children from birth to adolescence: a meta-analysis. JAMA. 2009; 302:2235–2242. [PubMed: 19934425]

Kinney HC. Human myelination and perinatal white matter disorders. J Neurol Sci. 2005; 228:190–192. [PubMed: 15694202]

Larroque B, Ancel P-Y, Marret S, Marchand L, André M, Arnaud C, Pierrat V, Rozé J-C, Messer J, Thiriez G, Burguet A, Picaud J-C, Bréart G, Kaminski M, EPIPAGE Study group. Neurodevelopmental disabilities and special care of 5-year-old children born before 33 weeks of gestation (the EPIPAGE study): a longitudinal cohort study. Lancet. 2008; 371:813–820. [PubMed: 18328928]

Leviton A, Allred E, Kuban KCK, Dammann O, O'Shea TM, Hirtz D, Schreiber MD, Paneth N, ELGAN Study Investigators. Early blood gas abnormalities and the preterm brain. Am J Epidemiol. 2010; 172:907–916. [PubMed: 20807736]

Limperopoulos C, Chilingaryan G, Guizard N, Robertson RL, Du Plessis AJ. Cerebellar injury in the premature infant is associated with impaired growth of specific cerebral regions. Pediatr Res. 2010; 68:145–150. [PubMed: 20389260]

Limperopoulos C, Soul JS, Gauvreau K, Huppi PS, Warfield SK, Bassan H, Robertson RL, Volpe JJ, du Plessis AJ. Late gestation cerebellar growth is rapid and impeded by premature birth. Pediatrics. 2005; 115:688–695. [PubMed: 15741373]

Maki T, Liang AC, Miyamoto N, Lo EH, Arai K. Mechanisms of oligodendrocyte regeneration from ventricular-subventricular zone-derived progenitor cells in white matter diseases. Front Cell Neurosci. 2013; 7:275. [PubMed: 24421755]

McCarthy KD, de Vellis J. Preparation of separate astroglial and oligodendroglial cell cultures from rat cerebral tissue. J Cell Biol. 1980; 85:890–902. [PubMed: 6248568]

Miller SP, Ferriero DM, Leonard C, Piecuch R, Glidden DV, Partridge JC, Perez M, Mukherjee P, Vigneron DB, Barkovich AJ. Early brain injury in premature newborns detected with magnetic resonance imaging is associated with adverse early neurodevelopmental outcome. J Pediatr. 2005; 147:609–616. [PubMed: 16291350]

Möbius W, Cooper B, Kaufmann WA, Imig C, Ruhwedel T, Snaidero N, Saab AS, Varoqueaux F. Electron microscopy of the mouse central nervous system. Methods Cell Biol. 2010; 96:475–512. [PubMed: 20869535]

Northam GB, Liégeois F, Chong WK, Wyatt JS, Baldeweg T. Total brain white matter is a major determinant of IQ in adolescents born preterm. Ann Neurol. 2011; 69:702–711. [PubMed: 21391229]

Pang Y, Cai Z, Rhodes PG. Effect of tumor necrosis factor-alpha on developing optic nerve oligodendrocytes in culture. J Neurosci Res. 2005; 80:226–234. [PubMed: 15765524]

Pang Y, Zheng B, Fan L-W, Rhodes PG, Cai Z. IGF-1 protects oligodendrocyte progenitors against TNFalpha-induced damage by activation of PI3K/Akt and interruption of the mitochondrial apoptotic pathway. Glia. 2007; 55:1099–1107. [PubMed: 17577243]

Parker J, Mitchell A, Kalpakidou A, Walshe M, Jung H-Y, Nosarti C, Santosh P, Rifkin L, Wyatt J, Murray RM, Allin M. Cerebellar growth and behavioural & neuropsychological outcome in preterm adolescents. Brain. 2008; 131:1344–1351. [PubMed: 18372312]

Di Penta A, Moreno B, Reix S, Fernandez-Diez B, Villanueva M, Errea O, Escala N, Vandenbroeck K, Comella JX, Villoslada P. Oxidative stress and proinflammatory cytokines contribute to demyelination and axonal damage in a cerebellar culture model of neuroinflammation. PLoS ONE. 2013; 8:e54722. [PubMed: 23431360]

Pinato L, da Silveira Cruz-Machado S, Franco DG, Campos LMG, Cecon E, Fernandes PACM, Bittencourt JC, Markus RP. Selective protection of the cerebellum against intracerebroventricular LPS is mediated by local melatonin synthesis. Brain Struct Funct. 2013

Raff MC, Lillien LE, Richardson WD, Burne JF, Noble MD. Platelet-derived growth factor from astrocytes drives the clock that times oligodendrocyte development in culture. Nature. 1988; 333:562–565. [PubMed: 3287177]

Reynolds R, Wilkin GP. Development of macroglial cells in rat cerebellum. II. An in situ immunohistochemical study of oligodendroglial lineage from precursor to mature myelinating cell. Development. 1988; 102:409–425. [PubMed: 2458224]

Richardson WD, Pringle N, Mosley MJ, Westermark B, Dubois-Dalcq M. A role for platelet-derived growth factor in normal gliogenesis in the central nervous system. Cell. 1988; 53:309–319. [PubMed: 2834067]

Ritter J, Schmitz T, Chew L-J, Bührer C, Möbius W, Zonouzi M, Gallo V. Neonatal hyperoxia exposure disrupts axon-oligodendrocyte integrity in the subcortical white matter. J Neurosci. 2013; 33:8990–9002. [PubMed: 23699510]

Riva D, Giorgi C. The cerebellum contributes to higher functions during development: evidence from a series of children surgically treated for posterior fossa tumours. Brain. 2000; 123(Pt 5):1051–1061. [PubMed: 10775549]

Sawada K, Saito S, Horiuchi-Hirose M, Mori Y, Yoshioka Y, Murase K. Dose-related cerebellar abnormality in rats with prenatal exposure to X-irradiation by magnetic resonance imaging volumetric analysis. Congenit Anom (Kyoto). 2013; 53:127–130. [PubMed: 23998266]

Schmitz T, Krabbe G, Weikert G, Scheuer T, Matheus F, Wang Y, Mueller S, Kettenmann H, Matyash V, Bührer C, Endesfelder S. Minocycline protects the immature white matter against hyperoxia. Exp Neurol. 2014; 254:153–165. [PubMed: 24491957]

Schmitz T, Ritter J, Mueller S, Felderhoff-Mueser U, Chew L-J, Gallo V. Cellular changes underlying hyperoxia-induced delay of white matter development. J Neurosci. 2011; 31:4327–4344. [PubMed: 21411673]

Spittle AJ, Doyle LW, Anderson PJ, Inder TE, Lee KJ, Boyd RN, Cheong JLY. Reduced cerebellar diameter in very preterm infants with abnormal general movements. Early Hum Dev. 2010; 86:1–5. [PubMed: 20004536]

Steinlin M. Cerebellar disorders in childhood: cognitive problems. Cerebellum. 2008; 7:607–610. [PubMed: 19057977]

Stoodley CJ, Schmahmann JD. Functional topography in the human cerebellum: a meta-analysis of neuroimaging studies. Neuroimage. 2009; 44:489–501. [PubMed: 18835452]

Stoodley CJ, Valera EM, Schmahmann JD. Functional topography of the cerebellum for motor and cognitive tasks: an fMRI study. Neuroimage. 2012; 59:1560–1570. [PubMed: 21907811]

Tang M, Alexander H, Clark RSB, Kochanek PM, Kagan VE, Bayir H. Minocycline reduces neuronal death and attenuates microglial response after pediatric asphyxial cardiac arrest. J Cereb Blood Flow Metab. 2010; 30:119–129. [PubMed: 19756023]

Tsuji M, Wilson MA, Lange MS, Johnston MV. Minocycline worsens hypoxic-ischemic brain injury in a neonatal mouse model. Exp Neurol. 2004; 189:58–65. [PubMed: 15296836]

Ueno M, Fujita Y, Tanaka T, Nakamura Y, Kikuta J, Ishii M, Yamashita T. Layer V cortical neurons require microglial support for survival during postnatal development. Nat Neurosci. 2013; 16:543–551. [PubMed: 23525041]

Volpe JJ. Cerebellum of the premature infant: rapidly developing, vulnerable, clinically important. J Child Neurol. 2009; 24:1085–1104. [PubMed: 19745085]

Vottier G, Pham H, Pansiot J, Biran V, Gressens P, Charriaut-Marlangue C, Baud O. Deleterious effect of hyperoxia at birth on white matter damage in the newborn rat. Dev Neurosci. 2011; 33:261–269. [PubMed: 21659719]

Wang SS-H, Kloth AD, Badura A. The Cerebellum, Sensitive Periods, and Autism. Neuron. 2014; 83:518–532. [PubMed: 25102558]

Wierzba-Bobrowicz T, Kosno-Kruszewska E, Gwiazda E, Lechowicz W. The comparison of microglia maturation in different structures of the human nervous system. Folia Neuropathol. 1998; 36:152–160. [PubMed: 9833392]

Wilson HC, Onischke C, Raine CS. Human oligodendrocyte precursor cells in vitro: phenotypic analysis and differential response to growth factors. Glia. 2003; 44:153–165. [PubMed: 14515331]

Xue M, Mikliaeva EI, Casha S, Zygun D, Demchuk A, Yong VW. Improving outcomes of neuroprotection by minocycline: guides from cell culture and intracerebral hemorrhage in mice. Am J Pathol. 2010; 176:1193–1202. [PubMed: 20110416]

Yan H, Rivkees SA. Hypoglycemia influences oligodendrocyte development and myelin formation. Neuroreport. 2006; 17:55–59. [PubMed: 16361950]

Main Points

Neonatal exposure to hyperoxia causes hypomyelination of the cerebellum. Reduced astroglial growth factor production but not microglial inflammation seems to contribute to oligodendroglial damage, and minocycline rescues oligodendroglia development in the cerebellum after hyperoxia.
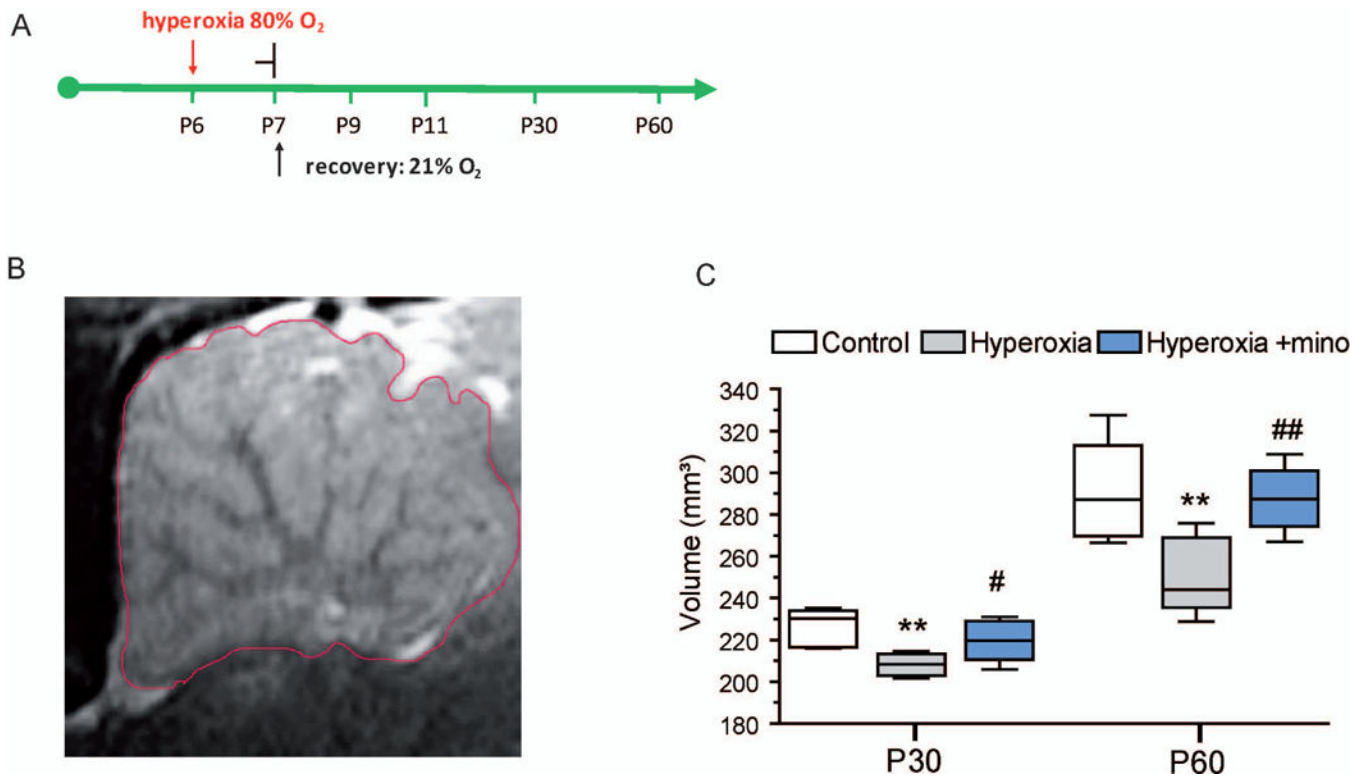
Figure 1. Reduced volume of the cerebellum after neonatal hyperoxia

(A) Timeline of exposure to hyperoxia (80 % O_2) for 24h from P6 to P7. Depending on the parameters investigated, recovery in room air followed thereafter for 2, 4, 23, and 53 days until P9, P11, P30, P60, respectively. (B, C) For determination of total volume of the cerebellum after neonatal hyperoxia, rat pups were exposed to 24h hyperoxia from P6 to P7 and returned into room air until young adult ages P30 and P60. MRI was then performed to obtain sagittal T2-weighted images. To capture the total expansion of the cerebellum, 25 sagittal images of a 0.5 mm slice thickness were taken. Calculation of cerebellum volumes was carried out with the program Analyze 5.0 (AnalyzeDirect, Inc.; Lenexa USA). Volumes were calculated by multiplying the summed cerebellum areas by the slice thickness, and the summed volume of these regions was used as the total cerebellar volume. B) shows a representative sagittal T2 image of the cerebellum of a P30 control rat. C) From age P30 to P60, control rats show a pronounced growth of the cerebellum. Rats exposed to 24h hyperoxia from P6 to P7 had significantly reduced cerebellar volumes at P30 and at P60 in comparison to normoxia control litters. Even though a growth progress from P30 to P60 can be observed in hyperoxia rats, too, volume deficit persists in comparison to controls. (C) Rats receiving minocycline during hyperoxia (Hyperoxia + mino) showed significantly higher cerebellar volumes at both at P30 and at P60 in comparison to hyperoxia rats without minocycline. (*$P<0.05$, ***$P<0.001$ vs. control; #$P<0.05$, ###$P<0.001$ vs. hyperoxia; ANOVA with consecutive t-test, n=8).
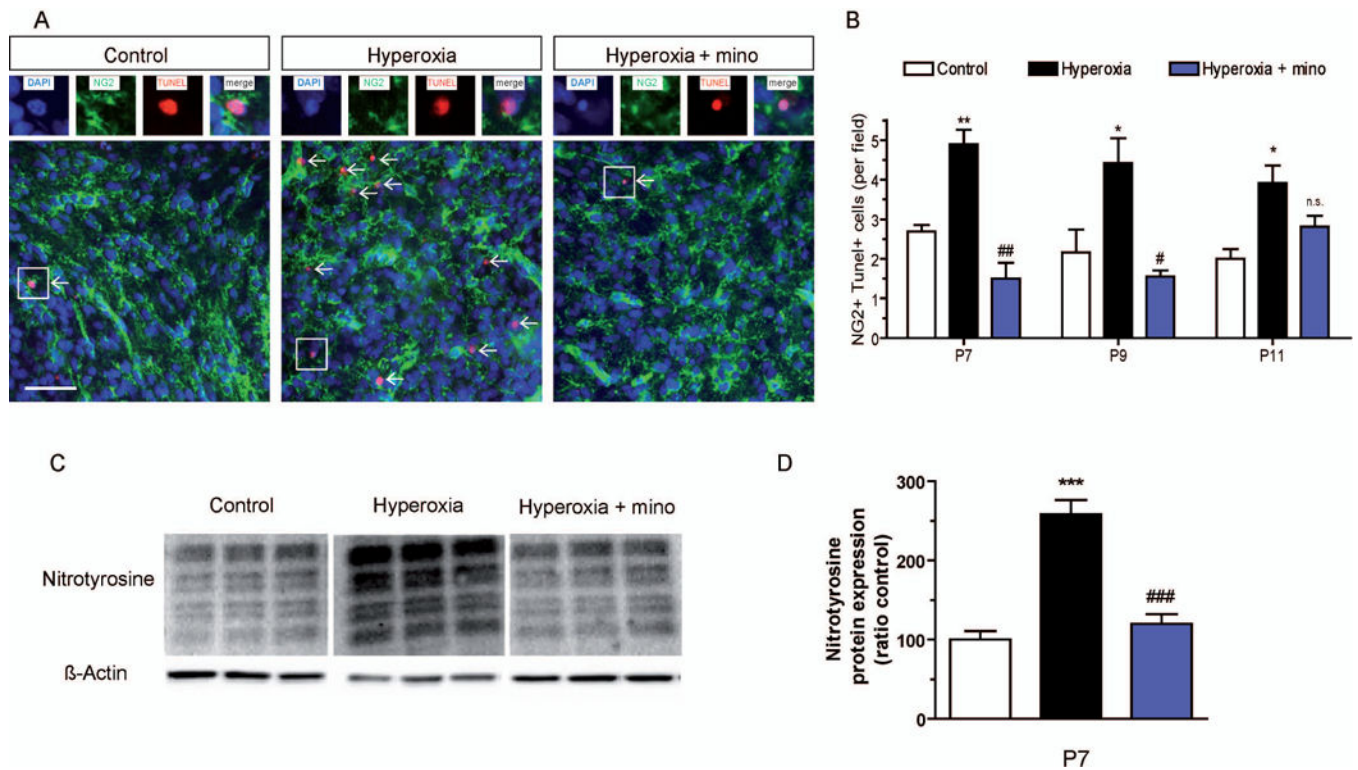
Figure 2. Apoptotic cell death and oxidative stress in the cerebellar white matter of P7 rats induced by hyperoxia

To investigate apoptotic cell death after 24h exposure to hyperoxia from P6 to P7 and after recovery at room air, we performed (A) immunohistochemistry of 10 μm cerebellar sections using NG2 to label oligodendroglial precursor cells (OPCs) of the white matter for co-stainings with TUNEL as a marker of apoptosis. (B) In the cerebellum of hyperoxic rats, TUNEL+ apoptosis in NG2+ OPCs was significantly increased immediately after hyperoxia at P7, and also after two days and four days recovery at P9 and P11, respectively. However, administration of minocycline during hyperoxia abolished pro-apoptotic effects of hyperoxia at P7 and P9. (C) To measure oxidative stress, Western blot for nitrotyrosine was performed with cerebellar protein samples at P7. (D) Hyperoxia induced nitrotyrosine production in the cerebellum by more than 2.5-fold, while minocycline blocked the increase of nitrotyrosine in hyperoxic rats. Scale bar = 50μm (***$P<0.001$, **$P<0.01$ and *$P<0.05$ versus controls; ###$P<0.001$, ##$P<0.01$ and #$P<0.05$ versus hyperoxia; ANOVA with consecutive t-test, (A, B) n=4; (C, D) n=6).
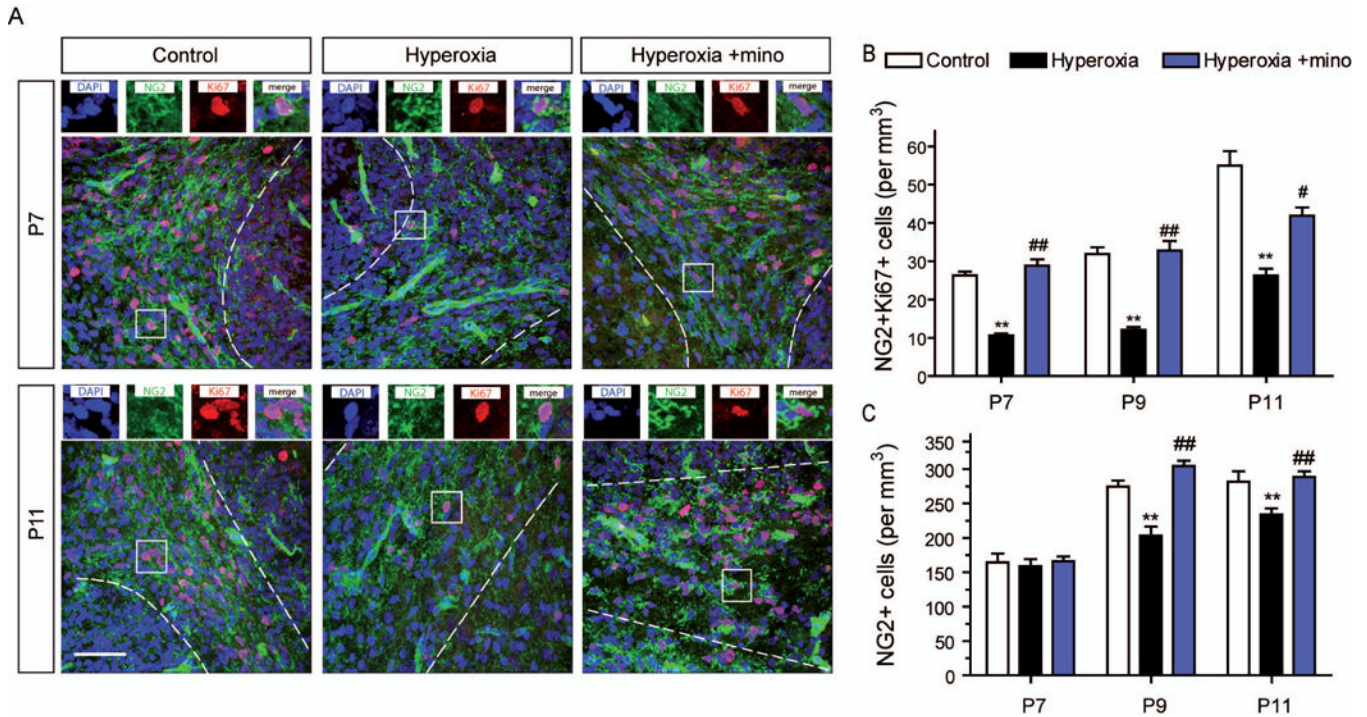
Figure 3. Proliferation of OPCs is reduced by hyperoxia and improved by minocycline

Immature oligodendroglia precursor cells undergo an intensive period of proliferation. To investigate this important step of oligodendroglia expansion we performed (A) immunohistochemistry of 10 μm cerebellar sections using antibodies against NG2 and the proliferation marker Ki67 to label proliferating OPCs at P7 immediately after 24h hyperoxia and after 2 and 4 days recovery in room air at P9 and at P11. (B) Numbers of NG2+Ki67+ OPCs in the cerebellar white matter were significantly reduced in rats after hyperoxia both at P7 and after recovery at P9 and P11. Administration of minocycline during hyperoxia abolished this reduction of OPC proliferation at all time points. (C) The total numbers of NG2+ cerebellar OPCs were not reduced after 24 h hyperoxia at P7. However, after recovery in room air at P9 and at P11, OPC numbers were significantly reduced in hyperoxia-experienced rats. Minocycline treatment during exposure to hyperoxia improved OPC numbers at both time points. Scale bar = 50μm. (**$P<0.01$ versus control, ##$P<0.01$ and #$P<0.05$, versus hyperoxia; ANOVA with consecutive t-test, n=4)
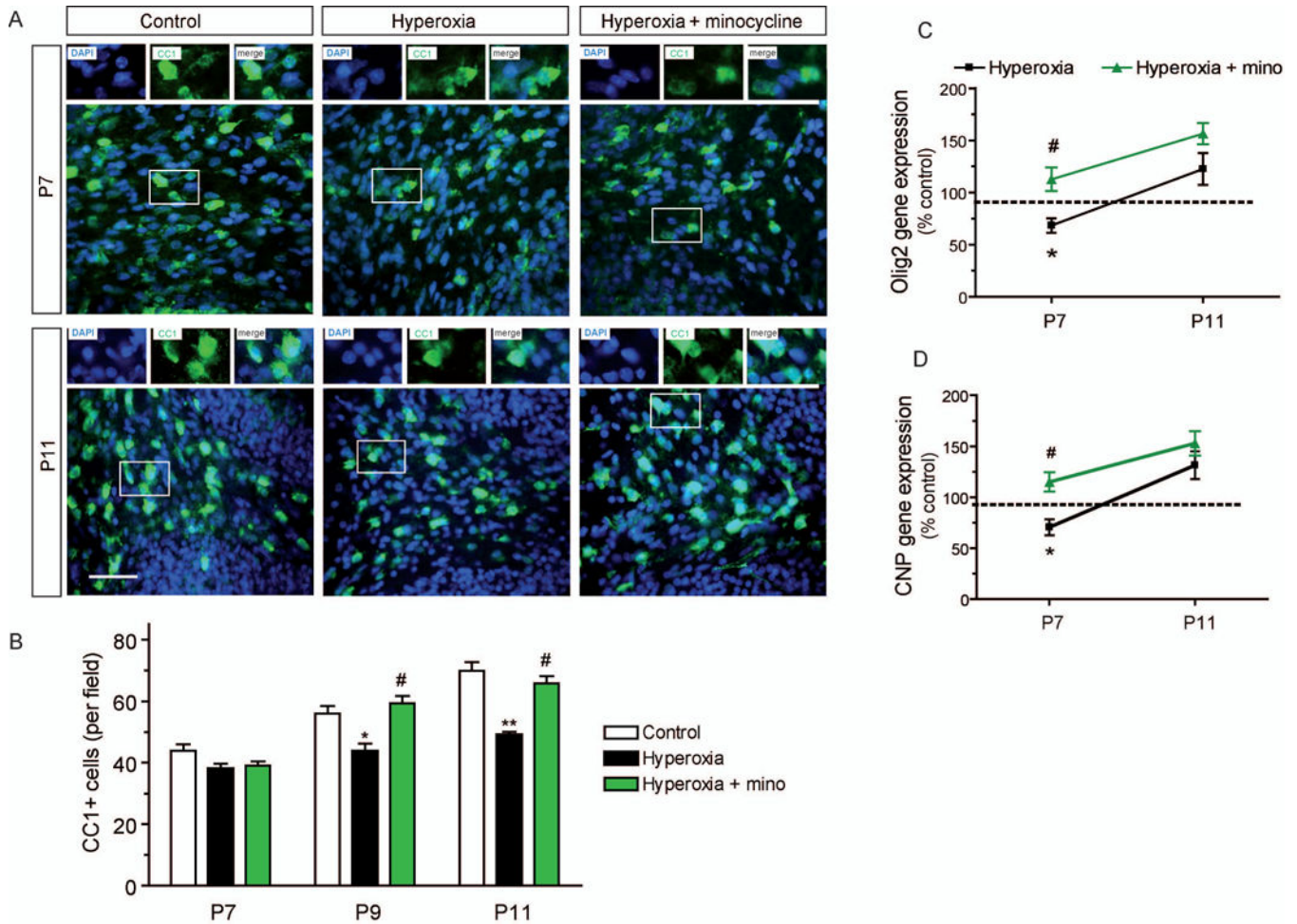
Figure 4. Perturbed maturation of oligodendroglial cells in the cerebellum after hyperoxia
(A) Immunohistochemistry of 10 μm cerebellar sections to label mature CC1+ oligodendrocytes at P7 immediately after exposure to hyperoxia followed by recovery in room air until P9 and P11. (B) Cell numbers of mature CC1+ oligodendrocytes in the cerebellar white matter were not reduced by hyperoxia at P7. At P9 and at P11, however, CC1+ cells were significantly reduced in rats after hyperoxia. Minocycline abolished the delay of oligodendroglial maturation. (C) Gene expression of the oligodendroglial transcription factor Olig2 was significantly decreased after hyperoxia at P7, whereas minocycline improved Olig2 expression. At P11, expression levels of Olig2 were increased in minocycline treated and untreated hyperoxia rats (n.s.). (D) Gene expression levels of oligodendroglial maturation marker CNP were significantly decreased after exposure to hyperoxia at P7 as measured by qPCR. Minocycline treatment abolished the reduction of CNP expression. At P11, CNP was increased both in minocycline treated and untreated hyperoxia rats (n.s.). Scale bar = 50μm (*P<0.05 and **P<0.01 versus control, ##P<0.01 and #P<0.05 versus hyperoxia; ANOVA with consecutive t-test, (A, B) n=4, (scale bar 50 μm); (C, D) n=6).
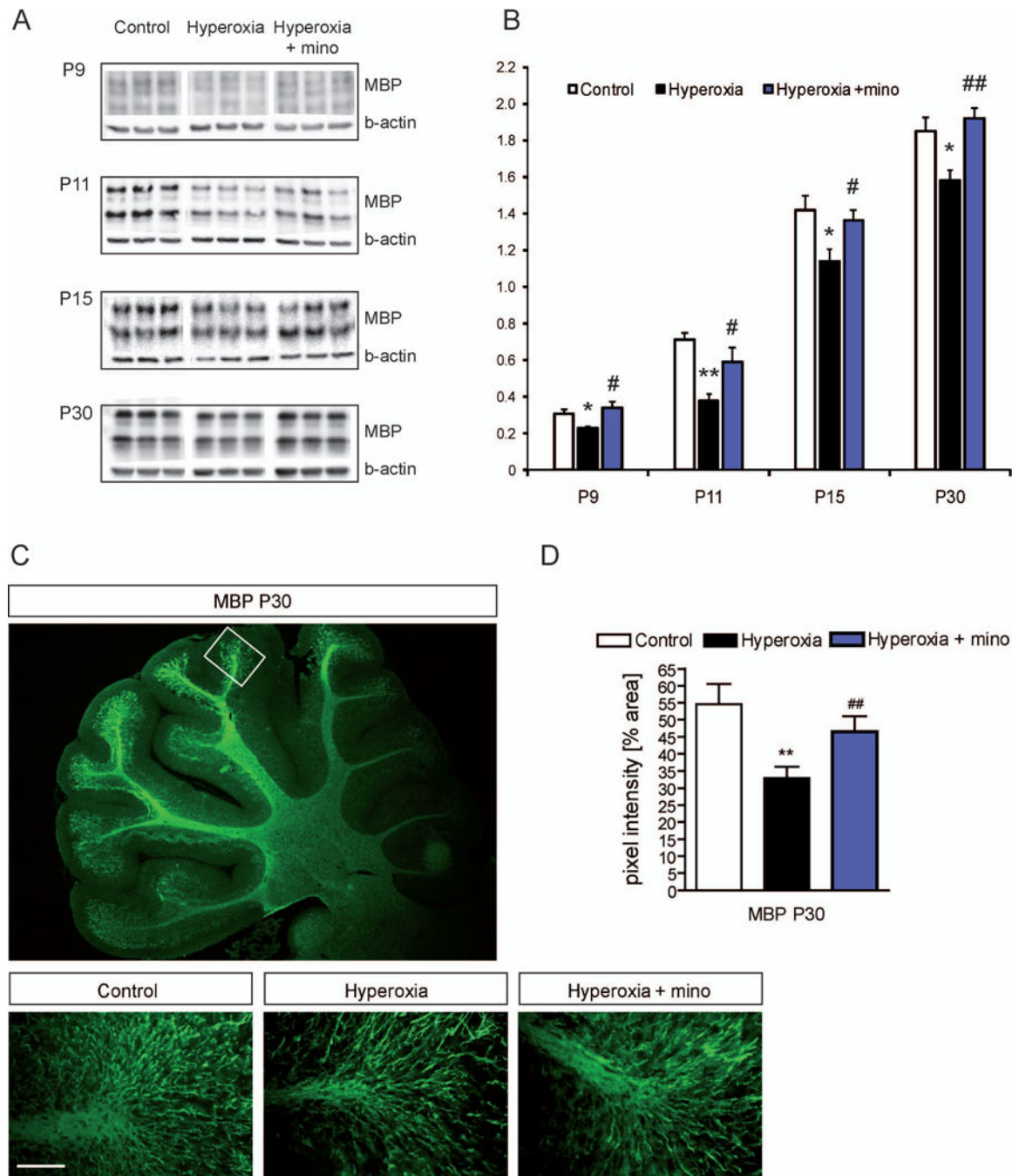
Figure 5. In the cerebellum, expression of myelin basic protein (MBP) is diminished by postnatal hyperoxia until young adult ages

To screen for myelination defects caused by hyperoxia we performed (A) Western blot analysis of MBP for myelin expression in cerebellar samples at P9, P11, P15 and P30 with β-actin for internal control. (B) Ratio of MBP to ß-actin protein expression. MBP was significantly diminished in developing rats at all time points. Minocycline treatment abolished the MBP deficits. (C) Immunohistochemistry of MBP in cerebellar sections at P30. (D) MBP pixel intensity at P30 was reduced in animals previously exposed to hyperoxia from P6 to P7. Minocycline increased MBP pixel intensity. Scale bar = 50μm

(*P<0.05 and **P<0.01 versus control, #P<0.05 and ##P<0.01 versus hyperoxia; ANOVA with consecutive t-test, (A, B) n=6; (C, D) n=4).
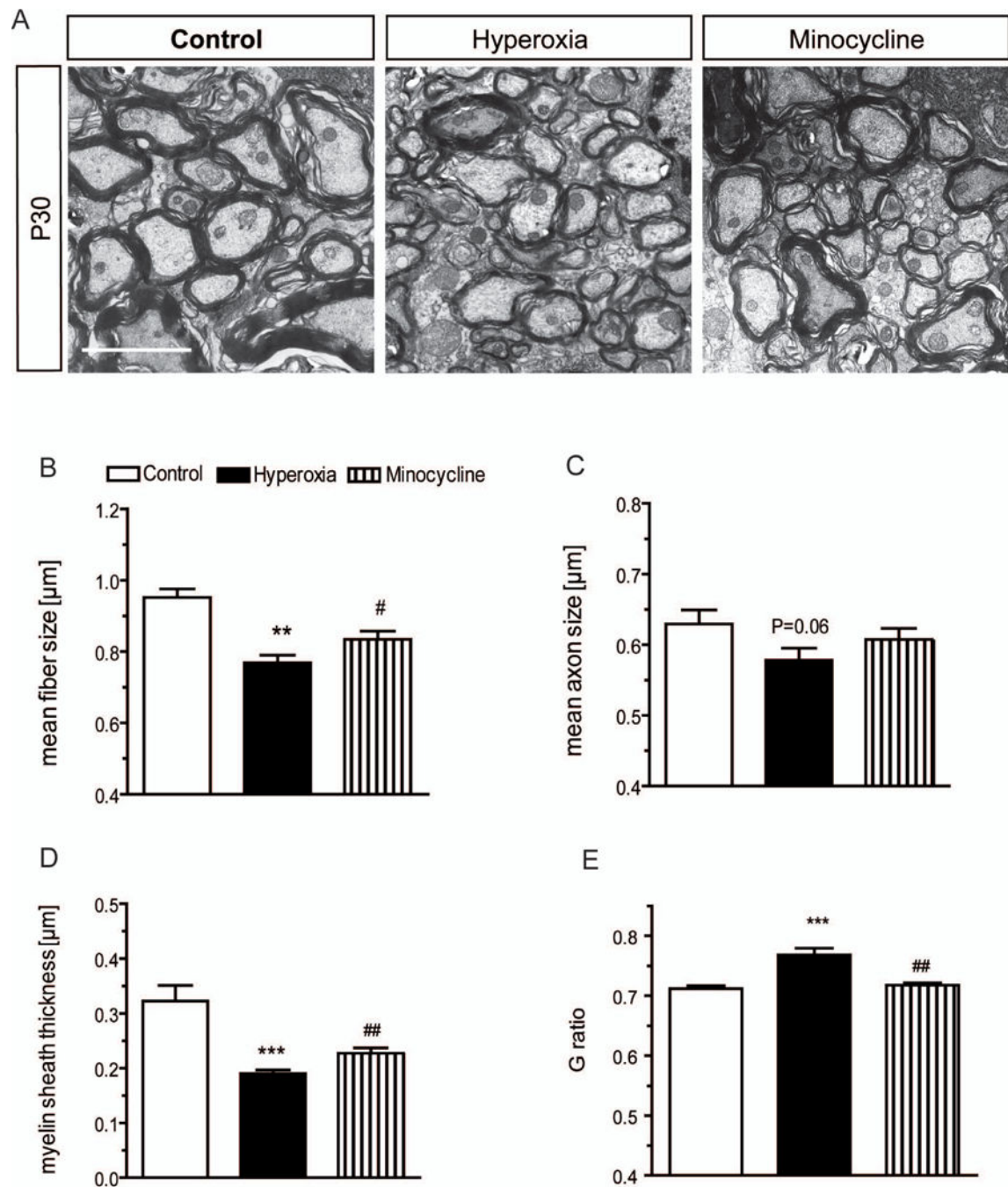
Figure 6. Electron microscopy of myelinated axons in the cerebellum

Electron microscopy was performed in sagittal sections of the cerebellum of P30 rats to analyze ultrastructure of myelinated axons (A). Mean size of fibers (B) (i.e., inner axon plus myelin sheath) and myelin sheath thickness (D) are significantly diminished after hyperoxia in comparison to control litters. (C) Mean size of axons tended to be lower after hyperoxia, indicating only borderline axonopathy. (E) In accordance with pronounced reduction of myelin sheath, G ratio is higher in radial images of axons obtained from hyperoxia rats. In animals that received minocycline during exposure to hyperoxia, fiber size and myelin

sheath thickness were significantly higher, and G ratio was significantly lower in comparison to hyperoxia-exposed rats without drug treatment (A-E). Images are taken at 10,000-fold magnification. Scale bar indicates 1 μm. (n=3 per group, 500 axons per animal; **$P<0.01$ and ***$P<0.001$ vs. control; #$P<0.05$, ##$P<0.01$ vs. hyperoxia; ANOVA with consecutive t-test).
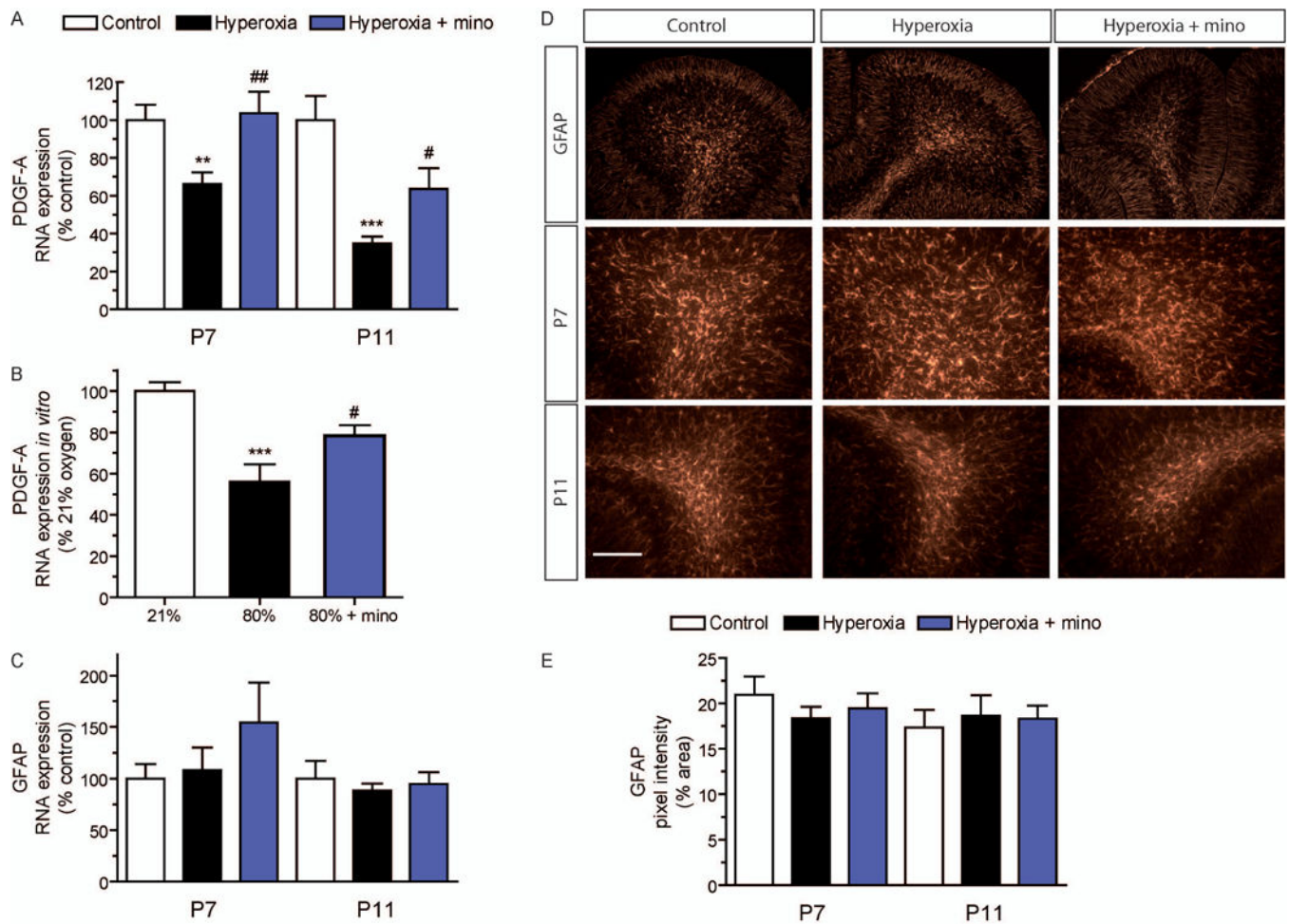
Figure 7. Downregulation of astroglial PDGF-A by hyperoxia

Interactions of different glial cell populations is indispensable for proper oligodendroglia development. PDGF-A secreted by astrocytes is known to stimulate the proliferation of immature OPCs. To analyze PDGF-A expression levels we performed qPCR analyses (A) of cerebellar samples at P7 and at P11. Exposure to hyperoxia downregulated the expression of PDGF-A, both at P7 and at P11. Minocycline treatment prevented the reduction of PDGF-A. (*P<0.05 and ***P<0.001 versus control, #P<0.05 and ##P<0.01 versus hyperoxia; ANOVA with consecutive t-test, n=6). (B) Expression analyses of PDGF-A in cultured cerebellar astrocytes. Primary rat astrocytes isolated from cerebellar mixed glial cultures showed a drastic decrease of PDGF-A expression when kept at 80% oxygen for 24h. The lack of PDGF-A expression was abolished by minocycline. (***P<0.001 versus 21% O_2, #P<0.05 versus 80% O_2; ANOVA with consecutive t-test, n=9). (C) GFAP gene expression of cerebellar samples at P7 and P11 was not affected by hyperoxia. (D) GFAP immunohistochemistry of cerebellar sections for astrocytes at P7 and P11. The shape of GFAP+ astrocytes was almost similar in all groups at both time points. (E) The pixel intensity of GFAP stainings did not differ between the experimental groups. Scale bar = 50μm

Table 1

Sequences of Oligonucleotides

Gene		Forward Primer	Reverse Primer	Probe
CNP	NM_012809.2	AGCTGTAGCACTGCATCAGAAATG	CAGTAATGGCCGACCTGATGT	CAGACACATACTTTACGCCAC
GFAP	NM_017009.2	TCTGGACCAGCTTACTACCAACAG	TGGTTTCATCTTGGAGCTTCTG	AGAGGGACAATCTCACACAG
HPRT	NM_012583.2	GGAAAGAACGTCTTGATTGTTGAA	CCAACACTTCGAGAGGTCCTTTT	CTTTCCTTGGTCAAGCAGTACAGCCCC
IGF1	NM_001082477.2	CGGACCAGAGACCCTTTGC	GCCTGTGGGCTTGTTGAAGT	Detected with SYBR Green
IL-lβ	NM_031512.2	CTCCACCTCAATGGACAGAACA	CACAGGGATTTTGTCGTTGCT	CTCCATGAGCTTTGTACAAG
IL-18	NM 019165.1	CGGAGCATAAATGACCAAGTTCTC	TGGGATTCGTTGGCTGTTC	TTGACAAAAGAAACCCGCCTG
01ig2	NM_001100557.1	TGCGCAAGCTCTCCAAGAT	TCTCGCTCACCAGTCTCTTCATC	CGAAACTACATCCTGATGCT
PDGF-A	NM_012801.1	TACCCCGGGAGTTGATCGA	CCCCTACGGAGTCTATCTCCAA	CTCGAAGTCAGATCCACAGC
TNFα	NM_012675.3	CCCCCAATCTGTGTCCTTCTAAC	CGTCTCGTGTGTTTCTGAGCAT	TAGAAAGGGAATTGTGGCTC